GEOPHYSICAL RESEARCH LETTERS, VOL. 24, NO.11, PAGES 1299-1302, JUNE 1, 1997

Imaging 3-D spherical convection models: What can seismic tomography tell us about mantle dynamics?

Charles Mégnin[1,3], Hans-Peter Bunge[2] Barbara Romanowicz[1,3] and Mark A. Richards [3]

Abstract.
We assess whether current global seismic tomography can resolve parameters characterizing mantle dynamics, in particular 1) a viscosity increase from the upper to the lower mantle, 2) an endothermic phase transition at the 670 km discontinuity, 3) heat flux across the core-mantle boundary and 4) the effect of the motion of rigid surface plates on the convection planform. We apply a 'linear seismic filter' to numerical convection models that incorporate the desired physical parameters, assuming that the shear velocity perturbations depend only on the convectively induced temperature variations. We show that the differences between the characteristic spectral patterns of convection models are preserved by the filtering process. Comparison with actual 3D seismic mantle models indicates that the effect of rigid plates dominates the spectral characteristics of the models. We estimate the effect of spatial aliasing of higher order structure into a lower order model, and find that the structure retrieved by inversion is more distorted by the effects of the aliasing than by those due to uneven ray coverage. This effect is strongest at shorter wavelengths and near the core-mantle boundary. We also find that the proper choice of radial smoothing parameters is crucial for detecting subtle signatures such as that of an endothermic phase transition at the 670 km discontinuity.

Introduction

Comparisons between 3-D spherical convection models and global mantle models derived from seismic tomography can help constrain physical parameters such as the amount of heat flux from the core, the Clapeyron slope of various phase transitions, the radial viscosity profile, and the effect of rigid plate motion at the Earth's surface on the convective planform of the mantle. Numerical models of mantle convection incorporating separately the effects of each of these parameters provide example 'signatures' of the corresponding physical phenomenon. Once identified, it is possible to seek the same signatures in models obtained from the inversion of seismic data. However, geodynamic models are generally developed at much greater spatial resolution than models obtained by seismic tomography. In order to compare the spectral characteristics of the two types of models, it is necessary to truncate the numerical model to the resolution of seismology *[e.g., Tackley et al., 1994]*.
Geodynamic models resulting from a simple truncation to low order differ in three fundamental ways from the seismological representation of the Earth. First the tomography represents a snapshot in time of what is modelled in numerical convection computations. Second, the structure derived from the latter has not been subjected to the limited sampling process of tomography dictated by limited ray coverage and frequency band of the waveforms used in the inversion. Finally, simple truncation to a lower order does not take into account the aliasing caused by the mapping of small scale Earth structure into long wavelength models.
The procedure we use bridges the difference in sampling between the two types of models by the application of a 'linear tomographic filter' to the geodynamic data. We show that the resulting filtered models are suitable for comparison with tomography, thus allowing a fairly realistic evaluation of the resolving power of seismic imaging in relation to various model parameters *[e.g., Johnson et al., 1993]*. We use spectral heterogeneity maps (SHM) representing the root mean square (rms) amplitude as a function of spherical harmonic degree and mantle depth to illustrate the models in wavenumber space. The degree of resolution is estimated by comparing radial rms amplitudes and by constructing SHMs of the difference between input and output models representing the structure unresolved by the seismic filter.

Method

We use as input models the results from eight demeaned 3-D spherical convection calculations by *Bunge et al., 1996, Bunge & Richards, 1996* (Figures 1 and 2, left columns). To circumvent the issue of time-dependence, we have selected models which have achieved statistical stability. We convert the temperature perturbations to shear wave velocity perturbations using a constant δT to $\delta ln(V_s)$ scaling. We wish to compute synthetic seismograms which duplicate the set of source-receiver pairs used by *Li & Romanowicz, 1996* (hereafter refered to as *L&R*) to develop the SH velocity model *SAW12D* using the nonlinear asymptotic coupling theory of *Li & Romanowicz, 1995* . The waveforms obtained can then be inverted for structure expanded to the desired spherical harmonic order. This process is nevertheless computationally intensive and it is well known that, under assumption of linearity, the model $\underline{\mathbf{m}}_{tomo}$ resulting from the inversion of synthetics generated through an input model $\underline{\mathbf{m}}_{conv}$ are related by

$$\underline{\mathbf{m}}_{tomo} = \underline{\underline{\mathbf{R}}}\,\underline{\mathbf{m}}_{conv} \qquad (1)$$

where $\underline{\underline{\mathbf{R}}}$ is the resolution matrix. The operator $\underline{\underline{\mathbf{R}}}$ thus

[1]Seismographic Station, [3]Department of Geology & Geophysics, University of California, Berkeley
[2]now at Institut de Physique du Globe, Paris, France

Paper number 97GL01256.
0094-8534/97/97GL-01256$05.00

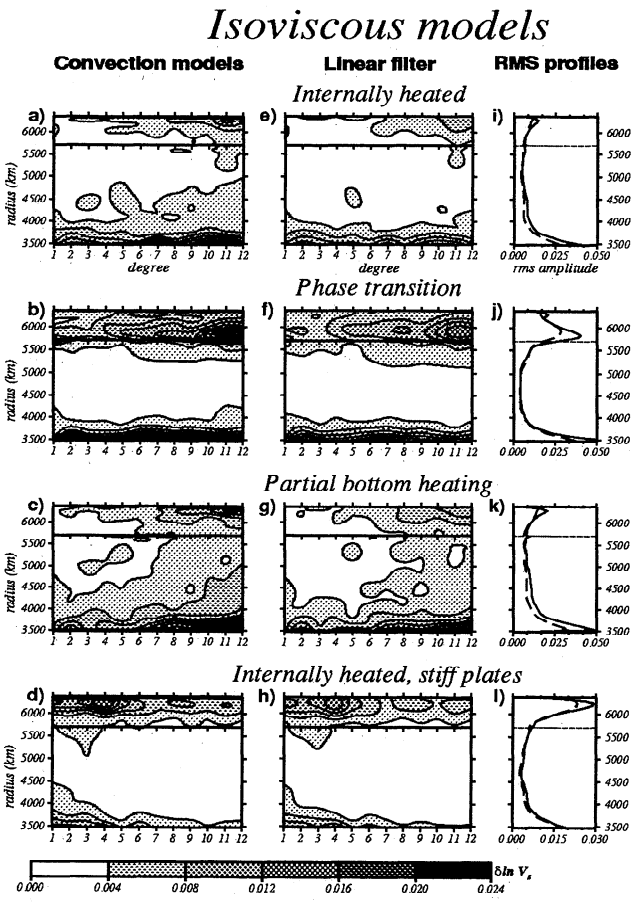

Figure 1. Isoviscous convection models (left) and the corresponding linear filters (middle). The isocontours represent the rms amplitude for each spherical harmonic degree (horizontal scale) at each radius (vertical scale). The 670km discontinuity is represented by a horizontal line. The corresponding radial rms profiles are given in the right column where the solid lines represent the input models and the dashed lines the inversion results.

acts as a 'linear tomographic filter' which, when applied to a particular model, reveals how the latter would be resolved by the tomography. The condition of linearity is however not pertinent to many waveform fitting techniques, which require inverting the data by the iterative linearization of the problem. The matrix $\underline{\underline{\mathbf{R}}}$ should therefore be model-dependent and its use theoretically justified solely in the vicinity of the model for which it was derived. Nevertheless, in the case of *SAW12D*, convergence was obtained after only a few iterations so that application of the method described above is expected (and has been verified) to constitute a viable first order approximation to the complete tomographic process. Here, we make use of the operator $\underline{\underline{\mathbf{R}}}$ derived in the last iteration of the computation of *SAW12D* to simulate the ray sampling by the transverse components of 9,626 body wave seismograms low-pass filtered at 32 seconds from 716 events and of 7,919 first and second orbit surface wave traces from 687 events low-pass filtered at 80 seconds, and the inversion of the resulting synthetic traces for structure up to spherical harmonic degree 12.

Results

We parametrize input and output models laterally using spherical harmonics up to degree 12, and radially in Legendre polynomials up to degree 5 in the upper mantle and up to degree 7 in the lower mantle, as in model *SAW12D*. The convection models *[Bunge et al., 1996, Bunge & Richards, 1996]* in the left column of Figure 1 correspond to an isoviscous mantle with a Rayleigh number of $1.1 * 10^8$ for the reference model (Figure 1 a)). Those in the left column of Figure 2 result from the introduction of a thirty-fold viscosity contrast in the lower mantle. The models at the top (Figures 1 & 2 a)) represent compressible flow and are purely internally heated. In the second row (Figures 1 & 2 b)), a strong endothermic phase transition with Clapeyron slope $\gamma = -4MPa/K$ is introduced. In the third row (Figures 1 & 2 c)), heat flux from the core is added to Figures 1 & 2 a), by the imposition of a constant temperature of T=3,450K at the core-mantle boundary (CMB), corresponding to 38% and 17% bottom heating for the isoviscous and the layered viscosity models, respectively. Finally, the bottom models (Figures 1 & 2 d)) are incompressible, internally heated, and incorporate the effects of the current motion of rigid plates at the surface. It has been shown by *Bunge & Richards (1996)* that the layered viscosity version of this model (Figure 2 d)) matches rather well the predominantly red heterogeneity pattern inferred from the geoid *[e.g.,*

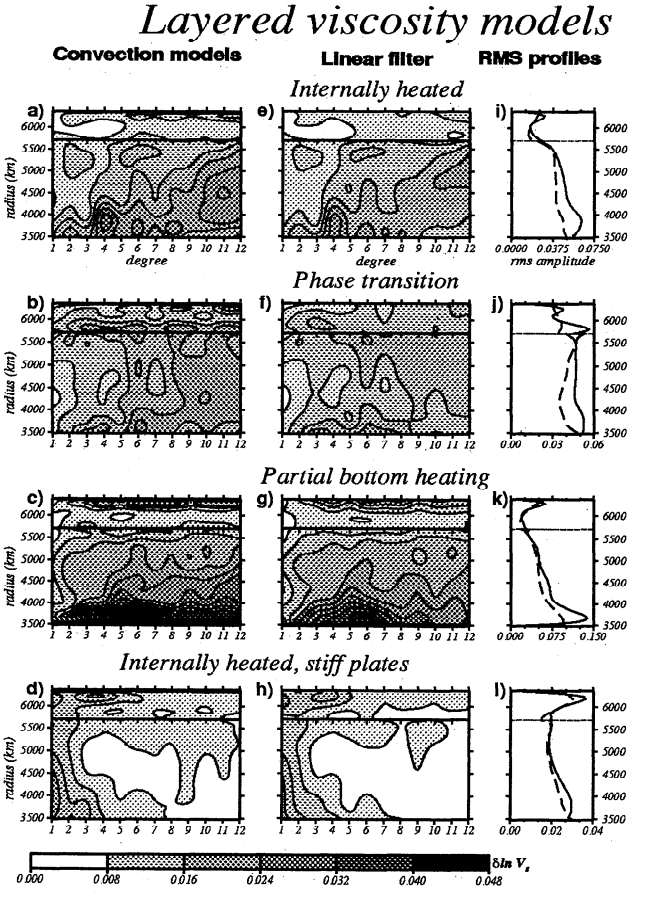

Figure 2. Same as Figure 1 for layered viscosity convection models.

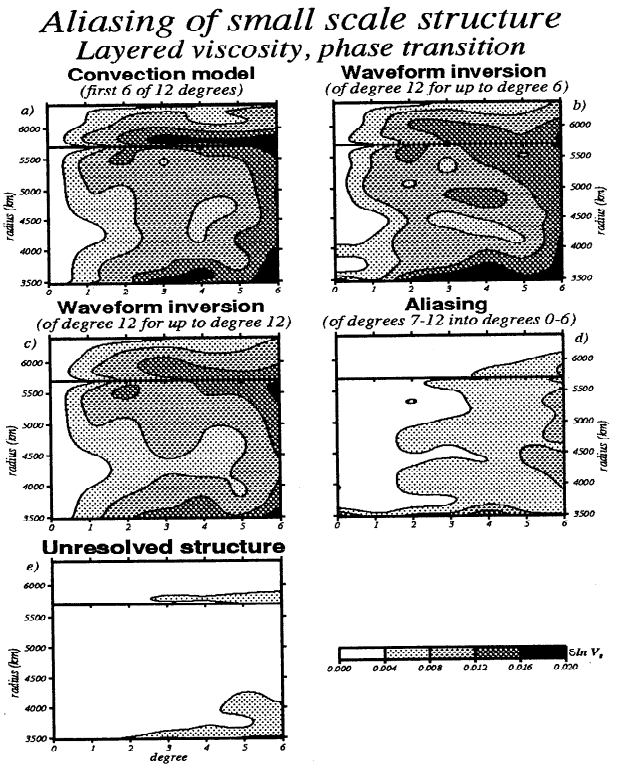

Figure 3. a) Layered viscosity model with a phase transition (first 6 of 12 degrees) ; b) Inversion for up to degree 6 of degree 12 model synthetics ; c) Inversion for up to degree 12 of degree 12 model synthetics ; d) difference between b) and c) giving a measure of the aliasing of high degree structure (degrees 7-12) into long wavelength models (degrees 0-6) ; e) difference between a) and c) giving a measure of the structure unresolved by the waveform inversion.

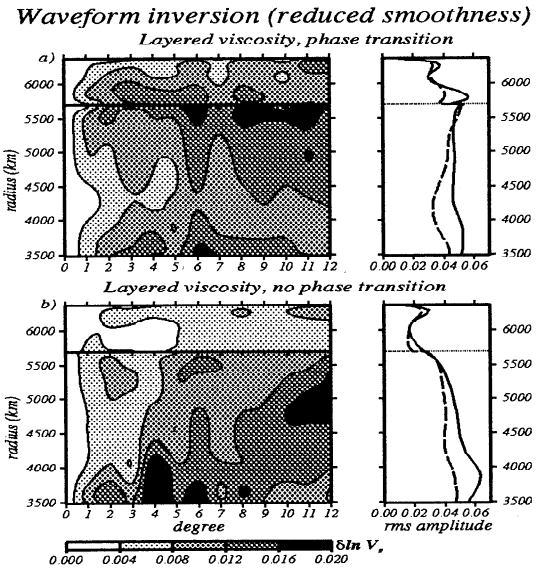

Figure 4. a) Inversion results for the layered viscosity model with a phase transition, with weak smoothness constraints across the 670 km discontinuity. In the right part of the figure, the solid line represents the rms of the input convection model and the dashed line that of the inverted model. b) Same as a) but with the internally heated-layered viscosity model. No spurious phase change signature is seen in this case.

Richards et al., 1988] and observed in current tomographic models *[e.g., Su et al., 1991]*.
In the center columns of Figures 1 and 2, we show the results of the application of relation (1) to the models in the left columns. The general spectral characteristics of the input models have been preserved despite the moderate damping in the rms amplitudes which results from a smallness constraint in the computation of *SAW12D*. The strong 'reddening' effect caused by the introduction of the viscosity layering shown in Figure 2 remains prominent in the tomographic models, as do the signatures of bottom heating above the CMB in the layered viscosity case (Figure 2 g)) and in the short wavelength planform of the isoviscous case (Figure 1 g)). On the other hand, the distinct spectral peaks present at degrees two and higher above the 670 km discontinuity for the layered viscosity model with a phase transition (Figure 2 b)) appear more attenuated, especially at high degrees (Figure 2 f) and j)). Figures 1 & 2 (i) - (l) further illustrate the attenuation of prominent short wavelength features in all models, resulting from the choice of a priori constraints favoring smooth features, in particular the transition from the upper to the lower mantle as discussed below. It is also interesting to note that the phase transition is better resolved in the isoviscous case (Figure 1 f)), reflecting the fact that, in the model of Figure 2, the seismic signal at that depth is dominated by the effect of the viscosity contrast across the phase boundary. Finally, the comparison between Figures 1 & 2 d) and h) shows that, apart from a slight amplitude attenuation, the spectral characteristics of the presence of surface plates are for the most part recovered by the application of the tomographic filter.

Aliasing

To investigate how short wavelength heterogeneity is 'seen' by long wavelength tomography, we generate synthetics through the layered viscosity convection model with a phase transition expanded up to degree 12 (figure 3 a)) and invert the traces for structure up to degree 6 (figure 3 b)) and up to degree 12 (figure 3 c)). The difference between the first 6 degrees of both models thus constitutes the amount of aliasing of degrees 7-12 into

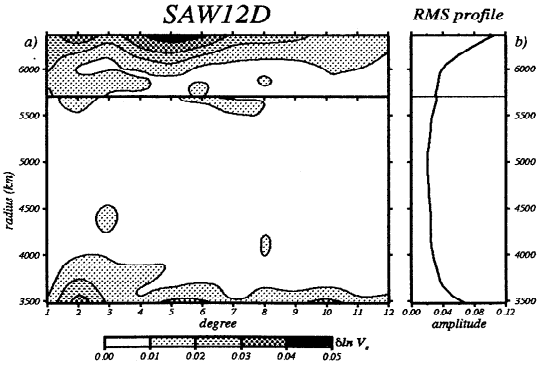

Figure 5. a) Spectral heterogeneity map of the seismic model SAW12D (Li & Romanowicz, 1996); b) Radial profile of the rms velocity fluctuations in SAW12D.

the long wavelength model (degrees 0-6) (figure 3 d)). It is seen that the aliasing increases with depth and peaks at the CMB where small structure contaminates all degrees up to and including the degree 0 term. The amplitude of the contamination furthermore exceeds that of the unresolved structure (figure 3 e)), in particular at higher degrees and increasingly with depth. Nevertheless, the dominant characteristics of the spectrum remain preserved in both inversions in spite of the fact that much of the power in the model is at degrees 7 and above (see figure 2 b)).

Effects of a priori constraints

We now test the hypothesis that the relative lack of resolution at the bottom of the upper mantle for the layered viscosity model with a phase transition is due to the a priori constraints imposed in the original inversion. We do this by relaxing the continuity constraint at 670 km and drastically reducing the damping on the radial curvature of the model. The SHM resulting from the waveform inversion with the set of reduced damping parameters is shown in Figure 4 a). We see that the peaks at all degrees are now recovered with an attenuation similar to that of the other models. For consistency, we verify that the signature of the phase transition is not an artifact of the new set of damping parameters. Figure 4 b) represents the linear filter corresponding to the new a priori constraints applied to the two-layered, internally heated model (Figure 2 a)). The inverted structure is seen to be largely unaffected by the new conditions (compare with Figures 2 e) & l)), and in particular does not spuriously produce the signature of a phase change. This experiment suggests that the imposition of a strong smoothness constraint between the upper and the lower mantle may impede the ability to image the effects of the phase change.

Discussion and conclusions

Our results indicate that tomography can resolve characteristic signatures of input convection models. There is substantial loss in rms amplitudes in particular for the layered viscosity model in the presence of a phase transition due to the imposition of a strong constraint of continuity across the 670 km boundary. The input structure is nevertheless recovered when that condition is relaxed.

The spectral characteristics of the whole mantle seismic model *SAW12D* (figure 5 a) & b)) most closely resemble those of figures 1 d) and 2 d) indicating that the effect of the stiff plates is dominant. There is not much evidence for the presence of a phase transition or bottom heating, but we have shown that the choice of smoothing parameters is critical for the recovery of such signatures. Inasmuch as the convection calculations are valid, this suggests that the somewhat ad hoc choice of a priori smoothing conditions used in inversions of whole mantle structure could be guided using experiments such as those presented here to gain further insight into the nature of mantle convection.

Acknowledgments. We thank Catherine Thoraval, Joe Durek and Xiang-Dong Li for fruitful discussions, and David Stevenson, Goran Ekström and an anonymous reviewer for insightful suggestions. This work was supported by IGPP-LANL, grant 97-704. Seismographic station contribution 97-2.

References

Bunge, H.P., M.A. Richards, and J.R. Baumgardner, A sensitivity study of 3-D spherical mantle convection at 10^8 Rayleigh number: Effects of depth-dependent viscosity, heating mode and an endothermic phase change, *in press, J. Geophys. Res.*, 1996.

Bunge, H.P. and M.A. Richards, The origin of long wavelength structure in mantle convection: effects of plate motions and visosity stratification, *in press,* Geophys. Res. Lett., 1996.

Johnson S., G. Masters, P.J. Tackley and G.A. Glatzmaier, How well can we resolve a convecting Earth with seismic data ? (abstract), Eos Trans. AGU, *74*(43), Fall Meeting suppl.,80, 1993.

Li, X.D. and B. Romanowicz, Comparison of global waveform inversions with and without considering cross-branch modal coupling, *Geophys. J. R. astr. Soc., 121*, 695-709, 1995.

Li, X.D. and B. Romanowicz, Global mantle shear-velocity model developed using nonlinear asymptotic coupling theory, *Geophys. J. R. astr. Soc., 101*, 22,245-22,272, 1996

Richards, M.A., B.H. Hager and N.H. Sleep, Dynamically supported geoid highs over hotspots: Observation and theory, *J. Geophys. Res., 93*, 7690-7708, 1988.

Su, W.-J. and A.M. Dziewonski, Predominance of long wavelength heterogeneity in the mantle, *Nature, 352*, 121-126, 1991.

Tackley, P.J., D.J. Stevenson, G.A. Glatzmaier and Gerald Schubert, Effects of multiple phase transitions in a three-dimensional spherical model of convection in Earth's mantle, *J. Geophys. Res., 99*, 15,877-15,901, 1994.

C. Mégnin & B. Romanowicz, Seismographic Station, University of California, Berkeley, CA
H.-P. Bunge, Institut de Physique du Globe de Paris, Paris, France
M. A. Richards, Department of Geology & Geophysics, University of California, Berkeley, CA

(received October 3, 1996; revised February 25, 1997; accepted April 21, 1997.)